https://doi.org/10.5194/acp-2019-660
Preprint. Discussion started: 14 August 2019

Atmospheric Chemistry and Physics Discussions

The evolution of cloud microphysics upon aerosol interaction at the summit of Mt. Tai, China

Jiarong Li[1], Chao Zhu[1], Hui Chen[1,*], Defeng Zhao[1], Likun Xue[2], Xinfeng Wang[2], Hongyong Li[2], Pengfei Liu[3,4,5], Junfeng Liu[3,4,5], Chenglong Zhang[3,4,5], Yujing Mu[3,4,5], Wenjin Zhang[6], Luming Zhang[7], Kai Li[7], Min Liu[7], Hartmut Herrmann[1,2,8], Jianmin Chen[1,4,9,*]

[1]Shanghai Key Laboratory of Atmospheric Particle Pollution and Prevention (LAP3), Department of Environmental Science and Engineering, Institute of Atmospheric Sciences, Fudan University, Shanghai 200438, China
[2]Environment Research Institute, School of Environmental Science and Engineering, Shandong University, Ji'nan 250100, China
[3]Research Center for Eco-Environmental Science, Chinese Academy of Sciences, Beijing 10085, China
[4]Center for Excellence in Urban Atmospheric Environment, Institute of Urban Environment, Chinese Academy of Science, Xiamen 361021, China
[5]University of Chinese Academy of Sciences, Beijing 100049, China
[6]State Environmental Protection Key Laboratory of Urban Ambient Air Particulate Matter Pollution Prevention and Control, College of Environmental Science and Engineering, Nankai University, Tianjin 300071, China
[7]Tai'an Municipal Ecological Environment Bureau, Shandong Tai'an Ecological Environment Monitoring Center, Tai'an 271000, China
[8]Leibniz Institute for Tropospheric Research, Leipzig, Germany
[9]Shanghai Institute of Eco-Chongming (SIEC), No.3663 Northern Zhongshan Road, Shanghai 200062, China

Corresponding to: Jianmin Chen (jmchen@fudan.edu.cn) and Hui Chen (hui_chen@fudan.edu.cn)

Abstract. The influence of aerosols, both natural and anthropogenic, remains a major area of uncertainty when predicting the properties and behaviour of clouds and their influence on climate. In an attempt to understand better the microphysical properties of cloud droplets, the aerosol-cloud interactions, and the corresponding climate effect during cloud life cycles in the North China Plain, an intensive observation took place from 17 June to 30 July 2018 at the summit of Mt. Tai. Cloud microphysical parameters were monitored simultaneously with number concentrations of cloud condensation nuclei (N_{CCN}) at different supersaturations, $PM_{2.5}$ mass concentrations, particle size distributions and meteorological parameters. Number concentrations of cloud droplets (N_C), liquid water content (LWC) and effective radius of cloud droplets (r_{eff}) show large variations among 40 cloud events observed during the campaign. Perturbations of aerosols will significantly increase the N_C of cloud droplets and shift cloud droplets toward smaller size ranges. Clouds in clean days are more susceptible to the change in concentrations of particle number (N_P). LWC shows positive correlation with r_{eff}. As N_C increases, r_{eff} changes from a trimodal distribution to a unimodal distribution. By assuming a cloud thickness of 100 m, we find that the albedo can increase 36.4% if the cloud gets to be disturbed by aerosols. This may induce a cooling effect on the local climate system. Our results contribute more information about regional cloud microphysics and will help to reduce the uncertainties in climate models when predicting climate responses to cloud-aerosol interactions.

https://doi.org/10.5194/acp-2019-660
Preprint. Discussion started: 14 August 2019

Atmospheric Chemistry and Physics Discussions

1. Introduction

Clouds represent a key process in the atmospheric hydrological cycle, which plays an important role in the atmospheric energy budget and significantly influence the global and regional climate (Chang et al., 2019;Zhang et al., 2004b). Clouds can be physically described by their liquid water contents (LWC), number concentrations of droplets (N_C) and effective radius of droplets (r_{eff}). These parameters may show small inter-annual variations for the same monitoring station (Möller et al., 1996), but they vary over a large range among different cloud types (Quante, 2004), cloud altitudes (Padmakumari et al., 2017;Zhao et al., 2018) and in different parts of a cloud (Deng et al., 2009). Anthropogenic aerosol emission increases the number of cloud condensation nuclei (CCN) and hence they increase the number of cloud droplets, which is called the "Twomey Effect" (Twomey, 1974).

The interactions between the clouds and the aerosols behave in complicated ways. Clouds efficiently remove aerosols by activating CCN to cloud droplets (Croft et al., 2010;Zhang et al., 2004a). The cloud processes can increase particles sizes (Herenz et al., 2018) and alter the CCN compositions through homogeneous and heterogeneous reactions (Roth et al., 2016). A recent study found that new particle formation near the cloud edges is probably attributable to the UV irradiation enhanced by the cloud reflection (Wehner et al., 2015). In addition, the increase in aerosol concentrations alters the cloud microphysics, which has been investigated for cloud processes under clean and polluted conditions. Padmakumari et al. (2017) found that the convective clouds over land were characterized by lower LWC and higher N_C due to the perturbation of pollution aerosol. Ground-based observations by radiometers during the summers of the U.S. Mid-Atlantic region revealed that cloud events with smaller droplets (< 7 μm) occurred more frequently in the polluted years than in the clean years (Li et al., 2017b). Ebmeier et al. (2014) also found a strong anti-correlation between the aerosol optical depth (AOD) and r_{eff} of the local clouds downwind from degassing volcanoes. In Brazil, the N_C of cumulus clouds was little influenced by the aerosol particles under polluted conditions, and only r_{eff} correlated well with LWC (Reid et al., 1999). The influence of pollution aerosols on the cloud microphysics is evident but varies for different regions and for different cloud types.

To evaluate better the influence of aerosols on the cloud microphysics the first indirect effect (FIE) has been widely applied (Lohmann and Feichter, 2005;McComiskey et al., 2009;Twohy et al., 2005). However, the arithmetic of FIE use different parameters to represent the aerosol loading, such as the number concentration of particles, the CCN concentration and the aerosol optical depth (AOD), which makes it difficult to compare the FIEs from different studies. Positive relationships between aerosol loading and r_{eff}, called the “anti-Twomey effect”, are widely observed, especially over land (Bulgin et al., 2008;Grandey and Stier, 2010;Tang et al., 2014;Wang et al., 2014).

The increase in the aerosol concentrations results in a longer cloud lifetime, thus producing large cloud fractions (Koren et al., 2005;Albrecht, 1989), and increasing cloud top height and cloud thickness (Fan et al., 2013), which further influence the regional and global climate (Rosenfeld, 2006;Seinfeld et al., 2016). The reduction in the precipitation or drizzle caused by

https://doi.org/10.5194/acp-2019-660
Preprint. Discussion started: 14 August 2019

Atmospheric Chemistry and Physics Discussions

the perturbation of aerosols (Andreae et al., 2004;Heikenfeld et al., 2019) delays the hydrological cycle (Rosenfeld, 2006). Through Model experiments with the Coupled Model Intercomparison Project phase 5 (CMIP5), Frey et al. (2017) found that the monthly mean cloud albedo of subtropical marine stratocumulus clouds increased with the addition of anthropogenic aerosols.

However, lacking knowledge of the size distributions of clouds and aerosols makes it difficult to evaluate the cloud microphysics in small-scale regions (Fan et al., 2016;Khain et al., 2015). Climate models incompletely capture the impact of cloud-aerosol interactions (Rosenfeld et al., 2014b). The unresolved process of cloud formation is one of the largest contributors to the uncertainties in the models (Stevens and Bony, 2013). In situ measurements of cloud microphysics by aircraft or on high-altitude monitoring sites have provided some additional information for insight into the cloud processes (Allan et al., 2008;Li et al., 2017a;Padmakumari et al., 2017;Van Pinxteren et al., 2016;Reid et al., 1999). Furthermore, we lack knowledge of the microphysical parameters of cloud at different stages, an analogous study by Mazoyer et al. (2019) found that different fog stages own varied relationships among microphysical parameters.

The summit of Mt. Tai is the highest point in the center of the North China Plain. Sufficient moisture in summer and dramatic temperature differences between day and night make it ideal for in situ orographic cloud monitoring (Li et al., 2017a). The summit of Mt. Tai is far away from anthropogenic emission sources on the ground. But high concentrations of inorganic ions in $PM_{2.5}$ (Zhou et al., 2009), abundant bacterial communities (Zhu et al., 2018), NH_3 and NO_x emissions form biomass burning (Chang et al., 2018) have been observed at the summit, thus one infers a strong anthropogenic influence. Previous studies of cloud samples collected at the same position showed high inorganic ion concentrations (Li et al., 2017a;Wang et al., 2011), which can be attributable to the perturbation of anthropogenic aerosol. In the present study in situ observations at the summit of Mt. Tai were conducted and used to study the evolution of cloud microphysics upon aerosol interaction within non-precipitating clouds. Two typical cloud processes are discussed in detail to elucidate the relationship of N_C, r_{eff} and LWC under clean or polluted conditions (indicated by N_P and N_{CCN}). This paper provides comprehensive information for the aerosol impact on the microphysical properties of orographic clouds. The albedo based on the observed data has been estimated for climate implication.

2. Experiments

2.1. Duration and site

From 17 June to 30 July 2018, 40 cloud events in total were monitored at the summit of Mt. Tai (Tai'an, China; 117°13'E, 36°18'N; 1545 m a.s.l.) which is located within the transportation channel between the North China Plain and the Yangtze River Delta (Shen et al., 2019). The altitude of Mt. Tai is close to 1.6 km, which is usually sited for the characteristic of particles inputting to clouds (Hudson, 2007).

https://doi.org/10.5194/acp-2019-660
Preprint. Discussion started: 14 August 2019

Atmospheric Chemistry and Physics Discussions

2.2. Cloud microphysical parameters

A Fog Monitor (Model FM-120, Droplet Measurement Technologies Inc., USA), a forward-scattering optical spectrometer with sampling flow of 1 m^3 min^{-1}, was applied in situ for real-time displaying size distributions of cloud droplets and computing N_C, LWC, median volume diameter (MVD) and effective diameter (ED) in the size range of 2 to 50 μm. The corresponding equations are:

$$N_C = \Sigma N_i,$$

$$\mathrm{LWC} = \frac{4\pi}{3}\Sigma N_i r_i^3 \rho_w,$$

$$\mathrm{MVD} = 2 \times \left(\frac{\Sigma N_i r_i^3}{\Sigma N_i}\right)^{\frac{1}{3}}$$

$$ED = 2 \times r_{eff} = 2 \times \Sigma n_i r_i^3 / \Sigma n_i r_i^2,$$

where N_i is the cloud number concentration at the ith bin, r_i represents the radius at the ith bin and ρ_w =1 g cm^{-3} stands for the density of liquid water. Droplets are categorized into 30 size bins with sampling resolution of 1 s. In this study, the cloud events are defined by the universally accepted threshold values in N_C and LWC, i.e., N_C > 10 # cm^{-3} and LWC > 0.001 g m^{-3} (Demoz et al., 1996). Too short cloud events with a duration < 15 minutes were excluded.

2.3. Aerosol size distribution

A Scanning Mobility Particle Sizer (SMPS, Model 3938, TSI Inc., USA) consisting of a Differential Mobility Analyzer (DMA, Model 3082, TSI Inc., USA) and a Condensation Particle Counter (CPC, Model 3775, TSI Inc., USA) was applied to monitor the size distributions of dehumidified aerosols through a PM_{10} inlet. The neutralized aerosols were classified by DMA to generate a monodisperse stream of known size according to their electrical mobility. The CPC placed downstream counts the particles and gives the number of particles with different sizes. In the present study, each scan was fixed at 5 min for every loop with a flow rate of 1.5 L min^{-1} sizing particles in the range of 13.6 - 763.5 nm in 110 size bins.

2.4. CCN number concentration

The N_{CCN} at certain supersaturations (ss) were quantified by a cloud condensation nuclei counter (Model CCN-100, DMT Inc., USA). The CCN counter was set at five ss values sequentially for 10 min each at 0.2 %, 0.4 %, 0.6 %, 0.8 % and 1.0 % with a full scan time resolution of 50 min. Data collected during the first 5 min of each ss was excluded since the CCN counter needs time for temperature stabilization after the change of ss. The ratio of sample flow to sheath flow was set at 1:10 with a total airflow of 500 ccm. The ss of CCN counter were calibrated before the campaign and checked at the end of the campaign with monodisperse ammonium sulfate particles of different sizes (Rose et al., 2008).

2.5. $PM_{2.5}$ concentrations and meteorological parameters

The $PM_{2.5}$ mass concentration was measured using a beta attenuation and optical analyzer (SHARP monitor, model 5030i,

https://doi.org/10.5194/acp-2019-660
Preprint. Discussion started: 14 August 2019

Atmospheric Chemistry and Physics Discussions

Thermo Scientific Inc., USA). Meteorological parameters including the ambient temperature (T, ℃), relative humidity (RH), wind speed (WS, m s^{-1}) and wind direction (WD, °) were provided by Shandong Taishan Meteorological Station at the same observation point.

2.6. The calculation of FIE

Aerosol first indirect effect can be evaluated based on different cloud microphysical properties (McComiskey et al., 2009;Feingold et al., 2001). In the present study, FIEs based either on the r_{eff} or on N_C were used claculated as

$$FIE_r = -\left(\frac{\Delta \ln r_{eff}}{\Delta ln N_P}\right)_{LWC},\ 0< FIE_r <0.33$$

$$FIE_N = -\left(\frac{\Delta \ln N_C}{\Delta ln N_P}\right),\ 0< FIE_N <1$$

Where N_P is applied as an proxy of aerosol amount (Zhao et al., 2012;Zhao et al., 2018).

2.7. The calculation of albedo

Cloud albedos can be calculated using the equations shown below (Seinfeld and Pandis, 2006). Assuming the cloud droplet size distribution can be approximated as monodisperse, the cloud optical thickness (τ_c) could be obtained by

$$\tau_c = h\left(\frac{9\pi LWC^2 N_c}{2\rho_w^2}\right)^{\frac{1}{3}}$$

where h is the thickness of the cloud and ρ_w is the density of cloud water.

For the nonabsorbing and horizontally homogeneous cloud, the cloud albedo (R_c) gives as (Lacis and Hansen, 1974)

$$Albedo = \frac{\sqrt{3}(1-g)\tau_c}{2+\sqrt{3}(1-g)\tau_c}$$

where g is the asymmetry factor. The radius of cloud droplets was much greater than the wavelength of visible light, hence g is 0.85. The equation before becomes to

$$Albedo = \frac{\tau_c}{\tau_c + 7.7}$$

3. Results and discussion

3.1. Overview of the cloud microphysics

The averaged N_C, LWC, and r_{eff} of the 40 cloud events at the summit of Mt. Tai varied over the ranges of 59–1519 # cm^{-3}, 0.01–0.59 g m^{-3} and 2.6–7.4 μm, respectively (Table S1). The number concentration of cloud droplets at Mt. Tai both in the present study and in 2014 can reach 2000-3000 # cm^{-3} (Li et al., 2017a), which is much higher than those values (with a range of 10–700 # cm^{-3}) for city fogs and convective and orographic clouds (Allan et al., 2008;Li et al., 2011;Padmakumari et al., 2017) (Table 1).

The microphysics of different clouds and fogs can generally be distinguished in a plot of r_{eff} (or MVD) against LWC. As

https://doi.org/10.5194/acp-2019-660
Preprint. Discussion started: 14 August 2019

Atmospheric Chemistry and Physics Discussions

illustrated in Fig. 1, the LWC increases as the altitude increases in order of city fogs, orographic clouds and convective clouds. It is consistent with the study by Penner et al. (2004) that LWC within clouds increases linearly with altitude. The increase of N_C and/or r_{eff} will result in the increase of LWC. But sometimes only one factor plays the determining role. Even though the maximum N_C in Shanghai fog were higher than those in Hyderaba clouds; the larger sizes of clouds in Hyderaba determined their higher LWC values. (Li et al., 2011;Padmakumari et al., 2017). When compared with previous orographic clouds, LWC at Mt. Tai appeared to show a larger range. We monitored the high values, which are comparable with convective clouds, and the low values, which are similar to city fogs.

As opposed to convective clouds studied by research aircraft, cloud events at Mt. Tai were monitored in a fixed location and more easily affected by locally transferred air mass. Therefore, it is very worthwhile to use Mt. Tai to study how the aerosols carried large amount of CCN influence cloud microphysics and even the cloud life cycle.

3.2. Analysis on typical cloud processes

Cloud process-1 (CP-1) lasted the longest, persisting 74 hours in the present study. Cloud droplets formed under a relatively stable (wind speed < 4 m s^{-1}) and clean ($PM_{2.5}$ ≈ 10.9 μg m^{-3}) set of circumstance accompanied by a slow increase of T_a (Fig. 2). During daytime, especially in the afternoon, the $PM_{2.5}$ mass concentration dramatically increased with little change in wind speed and wind direction. However, the cloud did not break up with the perturbation of particles. As opposed to CP-1, the eight cloud events of cloud process-2 (CP-2) occurred periodically under high $PM_{2.5}$ conditions (50.7 μg m^{-3} in average). When a cloud formed, $PM_{2.5}$ rapidly decreased to less than 7.0 μg m^{-3} due to cloud scavenge. At noon, both $PM_{2.5}$ and T_a increased. They pushed the minification of cloud droplet sizes (Rosenfeld et al., 2014a), decreased the ambient supersaturation, enhanced the evaporation of small droplets (Ackerman et al., 2004), and finally caused the cloud events to vanish (Mazoyer et al., 2019).

3.2.1. Evolution of cloud microphysics

Based on whether the perturbation of particles occurred, CP-1 was separated into four stages: SC1 (stage-clean 1); SP1 (stage-perturbation 1); SC2 (stage-clean 2); and SP2 (stage-perturbation 2) (Fig. 3b). The newly formed cloud droplets were characterized with low N_C (~306 # cm^{-3}), large r_{eff} (~9.44 μm) and high LWC/N_C (~1.9 mg $\#^{-1}$), which represents the contained water of each cloud droplet (Fig. 2f and 3b). During SP1 and SP2, the perturbation of particles rapidly scrambled the water of the formed cloud droplets causing a dramatic decrease of r_{eff} and LWC/N_C. The LWC/N_C and r_{eff} of CP-1 showed a strong positive relationship.

According to the regular changes of cloud microphysics, each cloud event of CP-2 was separated into activation stage (S1), collision-coalescence stage (S2), stable stage (S3), and dissipation stage (S4) (Fig. 3a). As opposed to CP-1, the newly formed cloud droplets during S1 were characterized by small size, high N_C and low LWC/N_C values (Fig. 2f and 3b). For example, about 2310 # cm^{-3} of cloud droplets can quickly form in the first 2 hours of CE-20. The r_{eff} of these droplets was

https://doi.org/10.5194/acp-2019-660
Preprint. Discussion started: 14 August 2019

Atmospheric Chemistry and Physics Discussions

smaller than 4.1 μm and LWC/N_C was about 0.2 mg #$^{-1}$. In going from S2 to S3, the strong collision-coalescence between cloud droplets caused the increase of both r_{eff} and LWC/N_C. In S4, N_C decreased with the reduction of r_{eff} and LWC/N_C.

3.2.2. Interactions between N_P, N_{CCN} and N_C

As mentioned above, CP-1 and CP-2 started with different $PM_{2.5}$ mass concentrations. Thus, the N_P and the N_{CCN} measured at ss = 0.2% ($N_{CCN,0.2}$) are discussed in detail to evaluate the different conditions before cloud onsets. Before the start of CP-1, less than 1110 # cm^{-3} of N_P existed in the atmosphere. Each cloud event in CP-2 occurred under high N_p (~ 5400 # cm^{-3}) and N_{CCN} (~ 2200 # cm^{-3}) conditions. We use N_{CCN} to N_P fractions ($N_{CCN,0.2}/N_p$, CCN activation ratio) to describe the ability of aerosols acting as CCN at ss 0.2%. As shown in Fig. 3b, $N_{CCN,0.2}/N_P$ exhibits some low values (e.g. < 0.2) yet it is always larger than 0.22 in CP-2.

Based on the plot of $N_{CCN,0.2}$ versus N_P, we compared the connection between N_P and N_{CCN} at Mt. Tai with that monitored at puy-de-Dome, France (Asmi et al., 2012). Even though the settled ss are different (0.2% at the summit of Mt. Tai and 0.24% at puy-de-Dome), most of the data points of CP-1 and CP-2 were distributed between the two recommended dashed lines (the visually defined boundaries in within most of the data are centered, Fig. 3c and 3d) by Asmi et al. (2012). Asmi et al. (2012) found that high N_{CCN}/N_C was accompanied with the elevated aerosol hygroscopicity parameter κ during winter when long-range transported polluted continental aerosol commonly occurred. At a given ss, Mazoyer et al. (2019) also found the CCN activation ratio was positively associated with κ during the ParisFog field campaigns. High κ values corresponded to high fractions of less volatile organic aerosols (Raatikainen et al., 2010) while low κ values can be caused by the local traffic and wood burning emissions (Hammer et al., 2014). This indicates that the different CCN activation ratios between CP-1 and CP-2 may be influenced by the chemical compositions of ambient aerosols.

During the studies of cloud physics, the viewpoint that the increase of N_P brings more CCN and further increases N_C is supported by in situ observations (Lu et al., 2007;Mazoyer et al., 2019) and modelling studies (Heikenfeld et al., 2019;Zhang et al., 2014). In contrast, some recent studies of fog which contains less LWC when compared with a cloud, suggest that the increase of N_P will decrease the ambient supersaturation and decrease droplet numbers (Boutle et al., 2018;Mazoyer et al., 2019). In the present study, both positive and negative relations between N_P and N_C have been observed. But they appeared at different cloud processes (e.g., N_P and N_C showed consistent variation in CP-1) and different stages of cloud events (e.g., An obviously inverse relation between N_P and N_C existed in S1 and S4 while N_P and N_C simultaneously decreased in S2). This emphasizes the importance of studying cloud microphysics during cloud cycles and explains why some monitored values of LWC and r_{eff} at Mt. Tai were comparable with city fogs as discussed in section 3.1.

3.2.3. Aerosol First Indirect Effect

To show the influence of N_P on cloud droplets, FIE_r and FIE_N of CP-1 and CP-2 are illustrated in Fig. 4 and Fig. S2. Except

https://doi.org/10.5194/acp-2019-660
Preprint. Discussion started: 14 August 2019

Atmospheric Chemistry and Physics Discussions

for the out-of-bound FIE_r values calculated with insufficient data points when LWC was larger than 0.7 g m^{-3}, FIE_r of 0.181 - 0.269 for CP-1 were always higher than those of 0.025–0.123 for CP-2 in corresponding narrow LWC ranges (Fig. S2). We verified this with FIE_N. Due to the limitation of the Fog Monitor, the number of cloud droplets smaller than 2 μm may be underestimated during the activation and dissipation stages (in S1 and S4) (Mazoyer et al., 2019). Thus, only the data for S2 and S3 were employed when calculating FIE_N of CP-2 (Fig. 4c). Even though the underestimation of N_C may also exist in CP-1, the FIE_N of CP-1 (0.544) was still higher than that of CP-2 (0.144). It indicated that cloud droplets formed in fewer background particle numbers are more sensitive to N_P. In the previous studies, both observation and modelling studies also found that FIE_r was higher under smaller aerosol amount conditions. Twohy et al. (2005) measured the equivalent FIEr of 0.27 in the California coast while Zhao et al. (2018) used satellite observations to attribute the value of 0.10-0.19 for convective clouds over Hebei, China. Using an adiabatic cloud parcel model, Feingold (2003) found FIE_r increased from 0.199 to 0.301 when N_P decreased to less than 1000 # cm^{-3}. By using the Community Atmospheric Model version 5 (CAM5), Zhao et al. (2012) also found high FIE_r values in the tropical West Pacific at Darwin (TWP) due to the low N_P in December, January, and February.

The positive FIE_r and FIE_N at Mt. Tai mean that the increase in N_P are accompanied by decreased r_{eff} and increased N_C. No negative FIE_r were found in the present study. Yuan et al. (2008) and Tang et al. (2014) applied AOD to represent aerosol loading and found negative FIE_r. Using the 2-D Goddard Cumulus Ensemble model (GCE), Yuan et al. (2008) found positive dependence of r_{eff} on AOD near coastlines of the Gulf of Mexico and the South China Sea. They hypothesized that it may be due to the increase of soluble organics particles (SSO), which is hydrophobic and will hinder the activation of particles, inducing giant CCN to absorb water vapour and therefor result in large AOD. Tang et al. (2014) revealed negative FIE values during observations over Eastern China and the surrounding sea. With Moderate Resolution Imaging Spectroradiometer (MODIS) observations, they found significant positive correlations between r_{eff} and AOD over inland regions. They explained that the negative FIE values are likely attributable to meteorological conditions which usually favours transport of both pollutants and water vapour from the South and Southeast China and leads to simultaneous increases in both AOD and r_{eff}.

An increase in LWC might reduce the FIE, especially at coastal sites (McComiskey et al., 2009;Zhao et al., 2012). However, weak variations of FIE_r with an increase of LWC were found at Mt. Tai. Zhao et al. (2012) represented that the low LWC effect on FIE may be due to the high aerosol loading during cloud processes.

3.2.4. Size distribution of cloud droplets and particles

To illustrate the evolution of the aerosol particles and the cloud droplets during the cloud processes, the size distributions of N_P and N_C during different cloud stages are respectively plotted in Fig. 5. For the lowest N_P during the cloud processes, SC1 and SC2 were characterized by the smallest N_C for the size bins of 2–13 μm but by the largest N_C for the largest size bin. This resulted in the larger r_{eff} in SC1 and SC2 as shown in Fig. 3b. This is in accordance with the study from Breon and Colzy (2000)

https://doi.org/10.5194/acp-2019-660
Preprint. Discussion started: 14 August 2019

Atmospheric Chemistry and Physics Discussions

that droplets are on average 2–3 μm larger in remote tropical oceans than over land where is affected by biomass burning. During two perturbation stages of SP1 and SP2 in CP-1 (Fig. 5b), large numbers of aerosols, especially those smaller than 150 nm, affected cloud events. This dramatically increased N_C of 5–10 μm and made N_C of SP1 and SP2 in different size bins all comparable with those of CP-2. Herenz et al. (2018) and Wegner et al. (2012) found that the influence of local pollution could initiate the number concentrations of particles smaller than 100 nm. Thus, the aerosols perturbed the cloud during CP-1 may likely come from local pollutions.

When compared with CP-1, the cloud events of CP-2 started with higher N_P. The spectra of size distributions of cloud droplets in CP-2 were narrower. More than 80% of the total measured cloud droplets were in the range of 5–10 μm (Fig. 5a). With the development of the cloud process, N_C in three size bins, [2, 5) μm, [5, 7) μm and [7,10) μm, showed a similar variation trend. The number concentrations of cloud droplets in S1 were the highest. In the two larger size bins which were [10, 13) μm and [13,50) μm, S2 had the highest N_C.

Except for the low N_P of particle smaller than 50 nm, N_P of other size bins were comparable before the cloud onset (Fig. 5a). When a cloud started, N_P of particles larger than 150 nm rapidly decreased by activation. Mertes et al. (2005) also found that particles centered at d_p = 200 nm could be efficiently activated to droplets while most Aitken mode particles remained in the interstitial phase. The number concentrations of particles in the size range of 50–150 nm were slightly influenced during cloud processes at Mt. Tai. The activated particles grew at the beginning of the cloud cycle would lower the surrounding supersaturation and to some extent limit further aerosol activation (Ekman et al., 2011). It caused the increase of N_P during S4.

3.3. Relations between LWC, R_{eff} and N_C

The hourly averaged LWC for CP-1 and CP-2 is plotted against corresponding r_{eff} in Fig. 6a. Large cloud droplets (r_{eff} > 8 μm) were observed in CP-1, while the r_{eff} for CP-2 varied narrowly in the range of 2.5–8 μm.

For the two relatively clean stages, SC1 and SC2, cloud droplets with r_{eff} > 8 μm can existed due to the weaker competition among droplets at lower N_{CCN} conditions. This has also been observed in the U.S. Mid-Atlantic region where cloud droplets with larger sizes are more easily formed with lower N_{CCN} (Li et al., 2017b). With the perturbation of particles during SP1 and SP2, the growth of cloud droplets was obviously limited at the same LWC level, which is referred to as the “Twomey effect” (Twomey, 1977). This is consistent with the illustration in Fig. 3 that cloud droplets in SP1 and SP2 were smaller.

Most cloud events in CP-2 can be clearly divided into four stages—incipient (S1), coagulation (S2), stabilization (S3), and dissipation (S4) (see also in section 3.2.3). Their corresponding LWC, r_{eff} and N_C are illustrated in the lower panel of Fig. 6a taking CE-20 as an example. During S1, the existing numerous CCN (Fig. 3a) were quickly activated to form cloud droplets. The newly formed droplets are characterized with small sizes but large numbers. They will suppress the beginning of collision-coalescence processes (Rosenfeld et al., 2014a) and may further significantly delay raindrop formation Qian et al. (2009). In S1, diffusional growth may play the important role of enlarging cloud droplets. Even though both N_C and r_{eff} increase, the

https://doi.org/10.5194/acp-2019-660
Preprint. Discussion started: 14 August 2019

Atmospheric Chemistry and Physics Discussions

increase in N_C (from 1188 # cm^{-3} to 2940 # cm^{-3}) instead of the growth of r_{eff} (from ~3.5 μm to ~4.5 μm) dominates the boost to the LWC. This is different from Mazoyer et al. (2019)'s result in that they found a clearly inverse relationship between the number and the size of droplets at the beginning of the first hour of fog events during the observation in suburban Paris. When compared with a cloud, fog is usually formed under conditions with less available liquid water (Fig. 1). It will limit the growth of fog droplets. The newly formed fog droplets will quickly compete for the water vapour, hinder the growth of droplets, and cause the inverse relationship with droplet number and size. At the beginning of S2, N_C reaches the maximum. The high N_C yields a great coalescence rate between cloud droplets. In addition, the coalescence processes have a positive feedback that will in turn accelerate this process (Freud and Rosenfeld, 2012) and cause the quick decrease of N_C (Fig. 3a). This makes cloud droplets in S2 characterized with larger sizes with lower number concentrations. LWC simply varies in a relatively narrow range (Fig. 6a). During S3, N_C is almost constant due to the formation, coagulation, and evaporation of the cloud droplets reaching a balance. Cloud droplets grow or shrink freely by water condensation or evaporation respectively. The r_{eff} is almost equal to the cube root of LWC. The increase of LWC values is mainly due to the increase in droplet sizes. During this stage, the concentration of soluble ions may decrease due to the increase of dilution from the increase of LWC (Li et al., 2017a). At the dissipation stage of S4, the clouds vanish due to mixing with the dry ambient air (Rosenfeld et al., 2014a). Both N_C and r_{eff} decline. It also illustrates in Fig. 5c that all the N_C of the five size bins of cloud droplets decrease in S4.

In order to investigate the variation of r_{eff} upon N_C, the distribution of r_{eff} was classified with different N_C ranges in Fig. 6b. For N_C < 1000 # cm^{-3}, r_{eff} displayed a trimodal distribution and concentrated on 3.5 μm (Peak-1), 4.9 μm (Peak-2) and 7.1 μm (Peak-3), respectively. Peak-1 corresponded to cloud droplets with low N_C, LWC, and r_{eff} values while the $N_{CCN0.2}$ was very high (Fig. 6c). These points represented cloud droplets in the incipient stage or the dissipation stage of cloud events where large numbers of CCN exist in the atmosphere. Peak-2 and Peak-3 represented the mature stages for cloud events with different environmental conditions. When compared with Peak-2, Peak-3 represented cloud droplets formed under a relatively cleaner atmosphere. In this circumstance, CCN were efficiently activated and had a lower concentration remaining in the atmosphere (Fig. 6c). The sufficient ambient water vapour accelerated the growth of the formed droplets, which were characterized with low N_C and LWC but large r_{eff}. Peak-2 also appeared for larger N_C ranges, whose distribution narrowed with slightly decreasing diameter mode. This indicated that the increase of N_C will decrease the droplet sizes. It reflects "Twomey effect" again in our study.

By assuming the thickness of cloud is constant at 100 m, the albedo can increase 36.4% when N_C increased from 352 # cm^{-3} to 2203 # cm^{-3}. Through studying marine stratocumulus clouds in the north-eastern Pacific Ocean, Twohy et al. (2005) also found that the increase of N_C by a factor of 2.8 would lead to 40% increase of albedo going from 0.325 to 0.458.

https://doi.org/10.5194/acp-2019-660
Preprint. Discussion started: 14 August 2019

Atmospheric Chemistry and Physics Discussions

4. Conclusion

From 17 June to 30 July 2018 in-situ observations of number concentrations and size distributions of aerosol and cloud droplets are employed to show aerosol-cloud interactions and corresponding indirect climate effect at the summit of Mt. Tai. Large variations of the characteristic values in terms of N_C, LWC and r_{eff} exist in different cloud processes. When compared with other orographic clouds, clouds at Mt. Tai are affected by air mass with high N_{CCN}. Clouds with small r_{eff} and LWC exist, which are comparable with urban fogs. Two typical cloud processes, CP-1 and CP-2, are applied to study the cloud-aerosol interactions based on the aerosol characteristics (especially N_p and N_{CCN}) before cloud onsets. For the CP-1, which forms in relatively clean conditions, water content is sufficient while N_{CCN} limits cloud droplet formation. The newly formed cloud droplets are characterized with low N_C but high LWC and large r_{eff}. When particle perturbation occurs, large numbers of N_{CCN} will compete water content with the formed cloud droplets and further dramatically decrease the LWC/N_C and r_{eff} values of cloud droplets. In CP-2, N_P before the cloud onset is high and N_{CCN} is sufficient. Water vapour becomes the limitation for cloud formation. Large numbers of small cloud droplets with low LWC/N_C form in the incipient stage of cloud events.

Both positive FIE_r and FIE_N values at Mt. Tai indicate that the increase of N_P will decrease r_{eff} and increase N_C of cloud droplets. FIE_r and FIE_N values are lower with higher N_P and N_{CCN}. This represents that the increase of N_P will more strongly decrease the size and increase the number of cloud droplets under the conditions of smaller aerosol amount. Particles larger than 150 nm can be efficiently activated to cloud droplets in the size range of 5–10 μm. In general, the size of cloud droplets positively correlates with LWC. But in different N_C ranges, the r_{eff} of cloud droplets show different distribution shapes. For N_C < 1000 # cm^{-3}, r_{eff} displayed a trimodal distribution. With the increase of N_C, a narrow distribution of r_{eff} appeared and concentrated between 3 μm and 5 μm.

For aerosols on the ground level, it is hard to transport to high altitudes just by convection. Theoretically, the air condition before the formation of cloud events in the high altitudes should resemble to the beginning of CP-1. However, Mt. Tai supplies a potential access for aerosol transportation. Even though the summit of Mt. Tai is far away from the polluted sources, the transported CCN changes the cloud microphysical properties and influences the cloud life cycle at Mt. Tai. The increased N_C and decreased r_{eff} dramatically increase the cloud albedo, which may further influence the regional climate in the North China Plain.

Until now, bulk and bin parameterizations of cloud microphysics are widely used in models. But both of them have their defects. Many bulk parameterizations lost the shape of the drop size distribution (Sant et al., 2013). Meanwhile the bin parameterizations are usually applied in relatively small domains for a short time period due to their expensive computation cost (Fan et al., 2016). What's more, discrepancy still exists between the widths of observed and simulated size distributions of cloud droplets (Grabowski and Wang, 2013). Our study supplies valuable information of cloud microphysics at the summit of Mt. Tai, which provides more data for modeling studies about the North China Plain in the future.

https://doi.org/10.5194/acp-2019-660
Preprint. Discussion started: 14 August 2019

Atmospheric Chemistry and Physics Discussions

Data availability

All data used to support the conclusion are presented in this paper. Additional data are available upon request. Please contact the corresponding authors (Jianmin Chen (jmchen@fudan.edu.cn) and Hui Chen (hui_chen@fudan.edu.cn)).

Author contribution.

JC, HC conceived the study. JL and CZ performed the field experiments and sampled cloud water. JL analysed the data and wrote the main manuscript text. JC, HC, DZ, CZ and HH revised the initial manuscript. LX, XW and HL supported the meteorological data and $PM_{2.5}$ mass concentration. PL, JL, CZ, YM and WZ assisted in instrument maintenance. LZ, KL and ML contributed to the organization and arrangement of the field observation. All of the authors discussed the results, and contributed to the final manuscript.

Competing interests.

The authors declare no conflict of interest.

Acknowledgement

This work was supported by the Ministry of Science and Technology of China (2016YFC0202700), Tai'an Research Project (SDTASJ2018-0761-00), National Natural Science Foundation of China (91843301，91743202, 41805091, 21806020)，and Marie Skłodowska-Curie Actions (690958-MARSU-RISE-2015).

References

Ackerman, A. S., Kirkpatrick, M. P., Stevens, D. E., and Toon, O. B.: The impact of humidity above stratiform clouds on indirect aerosol climate forcing, Nature, 432, 1014-1017, 10.1038/nature03174, 2004.

Albrecht, B. A.: Aerosols, cloud microphysics, and fractional cloudiness, Science, 245, 1227-1230, 10.1126/science.245.4923.1227, 1989.

Allan, J. D., Baumgardner, D., Raga, G. B., Mayol-Bracero, O. L., Morales-Garcia, F., Garcia-Garcia, F., Montero-Martinez, G., Borrmann, S., Schneider, J., Mertes, S., Walter, S., Gysel, M., Dusek, U., Frank, G. P., and Kraemer, M.: Clouds and aerosols in Puerto Rico - a new evaluation, Atmos. Chem. Phys., 8, 1293-1309, 10.5194/acp-8-1293-2008, 2008.

Andreae, M. O., Rosenfeld, D., Artaxo, P., Costa, A. A., Frank, G. P., Longo, K. M., and Silva-Dias, M. A. F.: Smoking rain clouds over the Amazon, Science, 303, 1337-1342, 10.1126/science.1092779, 2004.

Asmi, E., Freney, E., Hervo, M., Picard, D., Rose, C., Colomb, A., and Sellegri, K.: Aerosol cloud activation in summer and winter at puy-de-Dome high altitude site in France, Atmos. Chem. Phys., 12, 11589-11607, 10.5194/acp-12-11589-2012, 2012.

Boutle, I., Price, J., Kudzotsa, I., Kokkola, H., and Romakkaniemi, S.: Aerosol-fog interaction and the transition to well-mixed radiation fog, Atmos. Chem. Phys., 18, 7827-7840, 10.5194/acp-18-7827-2018, 2018.

https://doi.org/10.5194/acp-2019-660
Preprint. Discussion started: 14 August 2019

Breon, F. M., and Colzy, S.: Global distribution of cloud droplet effective radius from POLDER polarization meaurements, Geophys. Res. Lett., 27, 4065–4068, 2000.

Bulgin, C. E., Palmer, P. I., Thomas, G. E., Arnold, C. P. G., Campmany, E., Carboni, E., Grainger, R. G., Poulsen, C., Siddans, R., and Lawrence, B. N.: Regional and seasonal variations of the Twomey indirect effect as observed by the ATSR-2 satellite instrument, Geophys. Res. Lett., 35, 10.1029/2007gl031394, 2008.

Chang, Y., Zhang, Y., Li, J., Tian, C., Song, L., Zhai, X., Zhang, W., Huang, T., Lin, Y. C., Zhu, C., Fang, Y., Lehmann, M. F., and Chen, J.: Isotopic Constraints on the Atmospheric Sources and Formation of Nitrogenous Species in Biomass-Burning-Influenced Clouds, Atmos. Chem. Phys. Discuss., 2018, 1-27, 10.5194/acp-2018-1196, 2018.

Chang, Y., Guo, X., Tang, J., and Lu, G.: Aircraft measurement campaign on summer cloud microphysical properties over the Tibetan Plateau, Sci. Rep., 9, 10.1038/s41598-019-41514-5, 2019.

Croft, B., Lohmann, U., Martin, R. V., Stier, P., Wurzler, S., Feichter, J., Hoose, C., Heikkila, U., van Donkelaar, A., and Ferrachat, S.: Influences of in-cloud aerosol scavenging parameterizations on aerosol concentrations and wet deposition in ECHAM5-HAM, Atmos. Chem. Phys., 10, 1511-1543, 10.5194/acp-10-1511-2010, 2010.

Demoz, B. B., Collett, J. L., and Daube, B. C.: On the Caltech Active Strand Cloudwater Collectors, Atmos. Res., 41, 47-62, 10.1016/0169-8095(95)00044-5, 1996.

Deng, Z., Zhao, C., Zhang, Q., Huang, M., and Ma, X.: Statistical analysis of microphysical properties and the parameterization of effective radius of warm clouds in Beijing area, Atmos. Res., 93, 888-896, 2009.

Ebmeier, S. K., Sayer, A. M., Grainger, R. G., Mather, T. A., and Carboni, E.: Systematic satellite observations of the impact of aerosols from passive volcanic degassing on local cloud properties, Atmos. Chem. Phys., 14, 10601-10618, 10.5194/acp-14-10601-2014, 2014.

Ekman, A. M. L., Engstrom, A., and Soderberg, A.: Impact of Two-Way Aerosol-Cloud Interaction and Changes in Aerosol Size Distribution on Simulated Aerosol-Induced Deep Convective Cloud Sensitivity, J. Atmos. Sci., 68, 685-698, 10.1175/2010jas3651.1, 2011.

Fan, J., Leung, L. R., Rosenfeld, D., Chen, Q., Li, Z., Zhang, J., and Yan, H.: Microphysical effects determine macrophysical response for aerosol impacts on deep convective clouds, Proc. Natl. Acad. Sci. U. S. A., 110, E4581-E4590, 10.1073/pnas.1316830110, 2013.

Fan, J., Wang, Y., Rosenfeld, D., and Liu, X.: Review of Aerosol-Cloud Interactions: Mechanisms, Significance, and Challenges, J. Atmos. Sci., 73, 4221-4252, 10.1175/jas-d-16-0037.1, 2016.

Feingold, G., Remer, L. A., Ramaprasad, J., and Kaufman, Y. J.: Analysis of smoke impact on clouds in Brazilian biomass burning regions: An extension of Twomey's approach, J. Geophys. Res.: Atmos., 106, 22907-22922, 10.1029/2001jd000732, 2001.

https://doi.org/10.5194/acp-2019-660
Preprint. Discussion started: 14 August 2019

Feingold, G.: Modeling of the first indirect effect: Analysis of measurement requirements, Geophys. Res. Lett., 30, 10.1029/2003gl017967, 2003.

Freud, E., and Rosenfeld, D.: Linear relation between convective cloud drop number concentration and depth for rain initiation, J. Geophys. Res.: Atmos., 117, 13, 10.1029/2011jd016457, 2012.

Frey, L., Bender, F. A. M., and Svensson, G.: Cloud albedo changes in response to anthropogenic sulfate and non-sulfate aerosol forcings in CMIP5 models, Atmos. Chem. Phys., 17, 9145-9162, 10.5194/acp-17-9145-2017, 2017.

Grabowski, W. W., and Wang, L.-P.: Growth of Cloud Droplets in a Turbulent Environment, Annu. Rev. Fluid Mech., 45, 293-324, 10.1146/annurev-fluid-011212-140750, 2013.

Grandey, B. S., and Stier, P.: A critical look at spatial scale choices in satellite-based aerosol indirect effect studies, Atmos. Chem. Phys., 10, 11459-11470, 10.5194/acp-10-11459-2010, 2010.

Hammer, E., Gysel, M., Roberts, G. C., Elias, T., Hofer, J., Hoyle, C. R., Bukowiecki, N., Dupont, J. C., Burnet, F., Baltensperger, U., and Weingartner, E.: Size-dependent particle activation properties in fog during the ParisFog 2012/13 field campaign, Atmos. Chem. Phys., 14, 10517-10533, 10.5194/acp-14-10517-2014, 2014.

Heikenfeld, M., White, B., Labbouz, L., and Stier, P.: Aerosol effects on deep convection: the propagation of aerosol perturbations through convective cloud microphysics, Atmos. Chem. Phys., 19, 2601-2627, 10.5194/acp-19-2601-2019, 2019.

Herenz, P., Wex, H., Henning, S., Kristensen, T. B., Rubach, F., Roth, A., Borrmann, S., Bozem, H., Schulz, H., and Stratmann, F.: Measurements of aerosol and CCN properties in the Mackenzie River delta (Canadian Arctic) during spring-summer transition in May 2014, Atmos. Chem. Phys., 18, 4477-4496, 10.5194/acp-18-4477-2018, 2018.

Hudson, J. G.: Variability of the relationship between particle size and cloud-nucleating ability, Geophys. Res. Lett., 34, 10.1029/2006gl028850, 2007.

Khain, A. P., Beheng, K. D., Heymsfield, A., Korolev, A., Krichak, S. O., Levin, Z., Pinsky, M., Phillips, V., Prabhakaran, T., Teller, A., van den Heever, S. C., and Yano, J. I.: Representation of microphysical processes in cloud-resolving models: Spectral (bin) microphysics versus bulk parameterization, Rev. Geophys., 53, 247-322, 10.1002/2014rg000468, 2015.

Koren, I., Kaufman, Y. J., Rosenfeld, D., Remer, L. A., and Rudich, Y.: Aerosol invigoration and restructuring of Atlantic convective clouds, Geophys. Res. Lett., 32, 10.1029/2005gl023187, 2005.

Lacis, A. A., and Hansen, J. E.: Parameterization for absorption of solar-radiation in earths atmosphere J. Atmos. Sci., 31, 118-133, 10.1175/1520-0469(1974)031<0118:Apftao>2.0.Co;2, 1974.

Li, J., Wang, X., Chen, J., Chao, Z., and Herrmann, H.: Chemical composition and droplet size distribution of cloud at the summit of Mount Tai, China, Atmos. Chem. Phys., 17, 1-21, 2017a.

Li, P., Li, X., Yang, C., Wang, X., Chen, J., and Jr, J. L. C.: Fog water chemistry in Shanghai, Atmos. Environ., 45, 4034-4041,

https://doi.org/10.5194/acp-2019-660
Preprint. Discussion started: 14 August 2019

2011.

Li, S., Joseph, E., Min, Q., and Yin, B.: Multi-year ground-based observations of aerosol-cloud interactions in the Mid-Atlantic of the United States, J. Quant. Spectrosc. Radiat. Transfer, 188, 192-199, 10.1016/j.jqsrt.2016.02.004, 2017b.

Lohmann, U., and Feichter, J.: Global indirect aerosol effects: a review, Atmos. Chem. Phys., 5, 715-737, 10.5194/acp-5-715-2005, 2005.

Lu, C., Niu, S., Tang, L., Lv, J., Zhao, L., and Zhu, B.: Chemical composition of fog water in Nanjing area of China and its related fog microphysics, Atmos. Res., 97, 47-69, 2010.

Lu, M.-L., Conant, W. C., Jonsson, H. H., Varutbangkul, V., Flagan, R. C., and Seinfeld, J. H.: The Marine Stratus/Stratocumulus Experiment (MASE): Aerosol-cloud relationships in marine stratocumulus, J. Geophys. Res.: Atmos., 112, 10.1029/2006jd007985, 2007.

Mazoyer, M., Burnet, F., Denjean, C., Roberts, G. C., Haeffelin, M., Dupont, J. C., and Elias, T.: Experimental study of the aerosol impact on fog microphysics, Atmos. Chem. Phys., 19, 4323-4344, 10.5194/acp-19-4323-2019, 2019.

McComiskey, A., Feingold, G., Frisch, A. S., Turner, D. D., Miller, M. A., Chiu, J. C., Min, Q., and Ogren, J. A.: An assessment of aerosol-cloud interactions in marine stratus clouds based on surface remote sensing, J. Geophys. Res.: Atmos., 114, -, 2009.

Mertes, S., Galgon, D., Schwirn, K., Nowak, A., Lehmann, K., Massling, A., Wiedensohler, A., and Wieprecht, W.: Evolution of particle concentration and size distribution observed upwind, inside and downwind hill cap clouds at connected flow conditions during FEBUKO, Atmos. Environ., 39, 4233-4245, 10.1016/j.atmosenv.2005.02.009, 2005.

Möller, D., Acker, K., and Wieprecht, W.: A relationship between liquid water content and chemical composition in clouds, Atmos. Res., 41, 321-335, 1996.

Padmakumari, B., Maheskumar, R. S., Anand, V., and Axisa, D.: Microphysical characteristics of convective clouds over ocean and land from aircraft observations, Atmos. Res., 195, 62-71, 10.1016/j.atmosres.2017.05.011, 2017.

Penner, J. E., Dong, X. Q., and Chen, Y.: Observational evidence of a change in radiative forcing due to the indirect aerosol effect, Nature, 427, 231-234, 10.1038/nature02234, 2004.

Qian, Y., Gong, D. Y., Fan, J. W., Leung, L. R., Bennartz, R., Chen, D. L., and Wang, W. G.: Heavy pollution suppresses light rain in China: Observations and modeling, J. Geophys. Res.: Atmos., 114, 16, 10.1029/2008jd011575, 2009.

Quante, M.: The role of clouds in the climate system, J. Phys. IV, 121, 61-86, 10.1051/jp4:2004121003, 2004.

Raatikainen, T., Vaattovaara, P., Tiitta, P., Miettinen, P., Rautiainen, J., Ehn, M., Kulmala, M., Laaksonen, A., and Worsnop, D. R.: Physicochemical properties and origin of organic groups detected in boreal forest using an aerosol mass spectrometer, Atmos. Chem. Phys., 10, 2063-2077, 10.5194/acp-10-2063-2010, 2010.

Reid, J. S., Hobbs, P. V., Rangno, A. L., and Hegg, D. A.: Relationships between cloud droplet effective radius, liquid water

https://doi.org/10.5194/acp-2019-660
Preprint. Discussion started: 14 August 2019

content, and droplet concentration for warm clouds in Brazil embedded in biomass smoke, J. Geophys. Res.: Atmos., 104, 6145-6153, 1999.

Rose, D., Gunthe, S. S., Mikhailov, E., Frank, G. P., Dusek, U., Andreae, M. O., and Poeschl, U.: Calibration and measurement uncertainties of a continuous-flow cloud condensation nuclei counter (DMT-CCNC): CCN activation of ammonium sulfate and sodium chloride aerosol particles in theory and experiment, Atmospheric Chemistry and Physics, 8, 1153-1179, 10.5194/acp-8-1153-2008, 2008.

Rosenfeld, D.: Aerosol-cloud interactions control of earth radiation and latent heat release budgets, Space Sci. Rev., 125, 149-157, 10.1007/s11214-006-9053-6, 2006.

Rosenfeld, D., Andreae, M. O., Asmi, A., Chin, M., de Leeuw, G., Donovan, D. P., Kahn, R., Kinne, S., Kivekas, N., Kulmala, M., Lau, W., Schmidt, K. S., Suni, T., Wagner, T., Wild, M., and Quaas, J.: Global observations of aerosol-cloud-precipitation-climate interactions, Rev. Geophys., 52, 750-808, 10.1002/2013rg000441, 2014a.

Rosenfeld, D., Sherwood, S., Wood, R., and Donner, L.: Climate Effects of Aerosol-Cloud Interactions, Science, 343, 379-380, 10.1126/science.1247490, 2014b.

Roth, A., Schneider, J., Klimach, T., Mertes, S., van Pinxteren, D., Herrmann, H., and Borrmann, S.: Aerosol properties, source identification, and cloud processing in orographic clouds measured by single particle mass spectrometry on a central European mountain site during HCCT-2010, Atmos. Chem. Phys., 16, 505-524, 10.5194/acp-16-505-2016, 2016.

Sant, V., Lohmann, U., and Seifert, A.: Performance of a Triclass Parameterization for the Collision-Coalescence Process in Shallow Clouds, J. Atmos. Sci., 70, 1744-1767, 10.1175/jas-d-12-0154.1, 2013.

Seinfeld, J. H., and Pandis, S. N.: Atmospheric Chemistry and Physics: From Air Pollution to Climate Change, John Wiley & Sons, Inc., Hoboken, New Jersey, 2006.

Seinfeld, J. H., Bretherton, C., Carslaw, K. S., Coe, H., DeMott, P. J., Dunlea, E. J., Feingold, G., Ghan, S., Guenther, A. B., Kahn, R., Kraucunas, I., Kreidenweis, S. M., Molina, M. J., Nenes, A., Penner, J. E., Prather, K. A., Ramanathan, V., Ramaswamy, V., Rasch, P. J., Ravishankara, A. R., Rosenfeld, D., Stephens, G., and Wood, R.: Improving our fundamental understanding of the role of aerosol-cloud interactions in the climate system, Proc. Natl. Acad. Sci. U. S. A., 113, 5781-5790, 2016.

Shen, L., Wang, H., Yin, Y., Chen, J., and Chen, K.: Observation of atmospheric new particle growth events at the summit of mountain Tai (1534 m) in Central East China, Atmos. Environ., 201, 148-157, 10.1016/j.atmosenv.2018.12.051, 2019.

Stevens, B., and Bony, S.: What Are Climate Models Missing?, Science, 340, 1053-1054, 10.1126/science.1237554, 2013.

Tang, J. P., Wang, P. C., Mickley, L. J., Xia, X. G., Liao, H., Yue, X., Sun, L., and Xia, J. R.: Positive relationship between liquid cloud droplet effective radius and aerosol optical depth over Eastern China from satellite data, Atmos. Environ., 84, 244-253, 10.1016/j.atmosenv.2013.08.024, 2014.

https://doi.org/10.5194/acp-2019-660
Preprint. Discussion started: 14 August 2019

Twohy, C. H., Petters, M. D., Snider, J. R., Stevens, B., Tahnk, W., Wetzel, M., Russell, L., and Burnet, F.: Evaluation of the aerosol indirect effect in marine stratocumulus clouds: Droplet number, size, liquid water path, and radiative impact, J. Geophys. Res.: Atmos., 110, -, 2005.

Twomey, S.: Pollution and planetary albedo, Atmos. Environ., 8, 1251-1256, 10.1016/0004-6981(74)90004-3, 1974.

Twomey, S. A.: The Influence of Pollution on the Shortwave Albedo of Clouds, J. Atmos. Sci., 34, 1149-1154, 1977.

Van Pinxteren, D., Fomba, K. W., Mertes, S., Müller, K., Spindler, G., Schneider, J., Lee, T., Collett, J. L., and Herrmann, H.: Cloud water composition during HCCT-2010: Scavenging efficiencies, solute concentrations, and droplet size dependence of inorganic ions and dissolved organic carbon, Atmos. Chem. Phys., 15, 24311-24368, 2016.

Wang, F., Guo, J., Wu, Y., Zhang, X., Deng, M., Li, X., Zhang, J., and Zhao, J.: Satellite observed aerosol-induced variability in warm cloud properties under different meteorological conditions over eastern China, Atmos. Environ., 84, 122-132, 10.1016/j.atmosenv.2013.11.018, 2014.

Wang, Y., Guo, J., Wang, T., Ding, A., Gao, J., Yang, Z., Jr, J. L. C., and Wang, W.: Influence of regional pollution and sandstorms on the chemical composition of cloud/fog at the summit of Mt. Taishan in northern China, Atmos. Res., 99, 434-442, 2011.

Wegner, T., Hussein, T., Haemeri, K., Vesala, T., Kulmala, M., and Weber, S.: Properties of aerosol signature size distributions in the urban environment as derived by cluster analysis, Atmos. Environ., 61, 350-360, 10.1016/j.atmosenv.2012.07.048, 2012.

Wehner, B., Werner, F., Ditas, F., Shaw, R. A., Kulmala, M., and Siebert, H.: Observations of new particle formation in enhanced UV irradiance zones near cumulus clouds, Atmospheric Chemistry and Physics, 15, 11701-11711, 10.5194/acp-15-11701-2015, 2015.

Yuan, T., Li, Z., Zhang, R., and Fan, J.: Increase of cloud droplet size with aerosol optical depth: An observation and modeling study, J. Geophys. Res.: Atmos., 113, 10.1029/2007jd008632, 2008.

Zhang, L. M., Michelangeli, D. V., and Taylor, P. A.: Numerical studies of aerosol scavenging by low-level, warm stratiform clouds and precipitation, Atmos. Environ., 38, 4653-4665, 10.1016/j.atmosenv.2004.05.042, 2004a.

Zhang, X., Musson-Genon, L., Dupont, E., Milliez, M., and Carissimo, B.: On the Influence of a Simple Microphysics Parametrization on Radiation Fog Modelling: A Case Study During ParisFog, Boundary-Layer Meteorol., 151, 293-315, 10.1007/s10546-013-9894-y, 2014.

Zhang, Y., Rossow, W. B., Lacis, A. A., Oinas, V., and Mishchenko, M. I.: Calculation of radiative fluxes from the surface to top of atmosphere based on ISCCP and other global data sets: Refinements of the radiative transfer model and the input data, J. Geophys. Res.: Atmos., 109, 10.1029/2003JD004457 J. Geophys. Res. 2018/12/31 doi: 10.1029/2003JD004457, 2004b.

https://doi.org/10.5194/acp-2019-660
Preprint. Discussion started: 14 August 2019

Atmospheric Chemistry and Physics Discussions

Zhao, C., Klein, S. A., Xie, S., Liu, X., Boyle, J. S., and Zhang, Y.: Aerosol First Indirect Effects on Non-Precipitating Low-Level Liquid Cloud Properties as Simulated by CAM5 at ARM Sites, AGU Fall Meeting, 2012, 376-395,

Zhao, C., Qiu, Y., Dong, X., Wang, Z., Peng, Y., Li, B., Wu, Z., and Wang, Y.: Negative Aerosol-Cloud re Relationship from Aircraft Observations over Hebei, China, Earth Space Sci., 5, 2018.

Zhou, Y., Wang, T., Gao, X., Xue, L., Wang, X., Wang, Z., Gao, J., Zhang, Q., and Wang, W.: Continuous observations of water-soluble ions in PM 2.5 at Mount Tai (1534 m a.s.l.) in central-eastern China, J. Atmos. Chem., 64, 107-127, 2009.

Zhu, C., Chen, J., Wang, X., Li, J., Wei, M., Xu, C., Xu, X., Ding, A., and Collett, J. L., Jr.: Chemical Composition and Bacterial Community in Size-Resolved Cloud Water at the Summit of Mt. Tai, China, Aerosol Air Qual. Res., 18, 1-14, 10.4209/aaqr.2016.11.0493, 2018.

https://doi.org/10.5194/acp-2019-660
Preprint. Discussion started: 14 August 2019

Atmospheric Chemistry and Physics Discussions

List of Table and Figure Captions

Table 1: Comparison of clouds monitored at Mt. Tai with city fogs, convective clouds monitored by research aircrafts and other orographic clouds. Including sampling information (site, period and altitude), the range of $PM_{2.5}$ mass concentrations, the range of microphysical parameters (number concentrations of cloud droplets-N_c, liquid water content-LWC, median volume diameter-MVD, effective radius-r_{eff}) and the number of monitored clouds/cloud events/fog events.

Figure 1: Plots of effective radius (r_{eff}, a) or medium volume diameter (MVD, b) against liquid water content (LWC) for clouds and fogs from the literatures. The dashed and solid shapes indicated the airborne and land observation, respectively. The blue diamonds with error bars represented the average LWC and r_{eff} (or MVD) of 40 cloud events observed at Mt. Tai in the present study with corresponding ranges.

Figure 2: The monitoring information of CP-1 and CP-2. Including (a) Wind speed (WS, m s^{-1}) and wind direction (WD), (b) relative humidity (RH, %), ambient temperature (T_a, ℃) and dew point temperature (T_d, ℃) (c) $PM_{2.5}$ mass concentrations (μg m^{-3}) and volumn concentration of $PM_{0.8}$ (10^{-6} cm^3 cm^{-3}) (d) size distribution of particles (13.6-763.5 nm) and corresponding geometric mean radius (GMr_P) (e) size distribution of cloud droplets (2-50 μm) and corresponding geometric mean radius (GMr_C) (f) N_C and LWC of cloud droplets.

Figure 3. Variation of (a) N_C, N_p and $N_{CCN,0.2}$ (b) $N_{CCN,0.2}/N_P$ and LWC/N_C during CP-1 and CP-2. The plot of $N_{CCN,0.2}$ versus N_P (c) in CP-1 (d) in CP-2

Figure 4: The determination of FIE (a) based on r_{eff} (b) and (c) based on N_C.

Figure 5: Size distribution of particles and cloud droplets during CP-1 and CP-2. “NC” in (c) represents particle size distributions during cloudless period

Figure 6: The plot of LWC versus r_{eff} (a) in CP-1 and in CP-2 (b) under different N_C ranges (c) under different N_{CCN} (d) with the variation of albedo.

Figure 7: A schematic of cloud processes formed on different N_{CCN} and Np conditions.

Table 1: Comparison of clouds monitored at Mt. Tai with city fogs, convective clouds monitored by research aircrafts and other orographic clouds. Including sampling information (site, period and altitude), the range of $PM_{2.5}$ mass concentrations, the range of microphysical parameters (number concentrations of cloud droplets-N_c, liquid water content-LWC, median volume diameter-MVD, effective radius-r_{eff}) and the number of monitored clouds/cloud events/fog events.

Sampling Site	Period	Altitude (m a.s.l)	$PM_{2.5}$ ($\mu g\ m^{-3}$)	N_C ($\#\ cm^{-3}$)	LWC ($g\ m^{-3}$)	MVD (μm)	r_{eff} (μm)	Number of clouds/cloud events/fog events	Reference
City Fog									
Shanghai, China	Nov. 2009	7	-	11-565	0.01-0.14	5.0-20.0	-	1	(Li et al., 2011)
Nanjing, China	Dec. 2006- Dec. 2007	22	0.03[a]-0.60[a]	-	2.69e^{-3}-0.16	-	1.6[b]-2.7[b]	7	(Lu et al., 2010)
Convective Clouds									
Amazon Basin/cerrado reCompagions, Brazil	Aug.-Sept. 1995	90-4000	-	-	0[d]-2.10[d]	-	2.8[d]-9.2[d]	>1000	(Reid et al., 1999)
Hyderaba - The Bay of Bengal, India	29th Oct. 2010	1300-6300		10[d]-380	0[d]-1.80		3.8[d]-17.0	1	(Padmakumari et al., 2017)
Orographic clouds									
Mt. Schmücke, Germany	Sep.-Oct. 2010	937	-	-	0.14-0.37	-	5.7-8.7	8	(Van Pinxteren et al., 2016)
East Peak Mountain, Puerto Rico	Dec. 2004	1040	-	193-519	0.24-0.31	14.0-20.0	-	2	(Allan et al., 2008)
Mt. Tai, China	Jul.-Aug. 2014	1545	11.1-173.3	4-2186	0.01-1.52	1.6-43.0	0.8-18.9	24	Unpublished data from (Li et al., 2017a)
Mt. Tai, China	Jun.-Jul. 2018	1545	1.2-127.1	10-3163	1.01e^{-3}-1.47	4.4-25.0	2.4-13.4	40	This study
Mt. Tai, China (CP-1[c])	10th – 13th Jul. 2018	1545	1.3-40.7	11-2470	1.12e^{-3}-1.47	4.6-17.4	2.5-10.7	12	This study
Mt. Tai, China (CP-2[c])	13th – 20th Jul. 2018	1545	1.2-66.2	10-3163	1.03e^{-3}-1.10	4.6-13.5	2.4-7.9	12	This study

[a] Represents the mass concentrations of PM_{10}. [b] Represents the range of averaged radium. [c] Two cloud processes which are detailedly discussed in this study. [d] Values were read from the graphs.

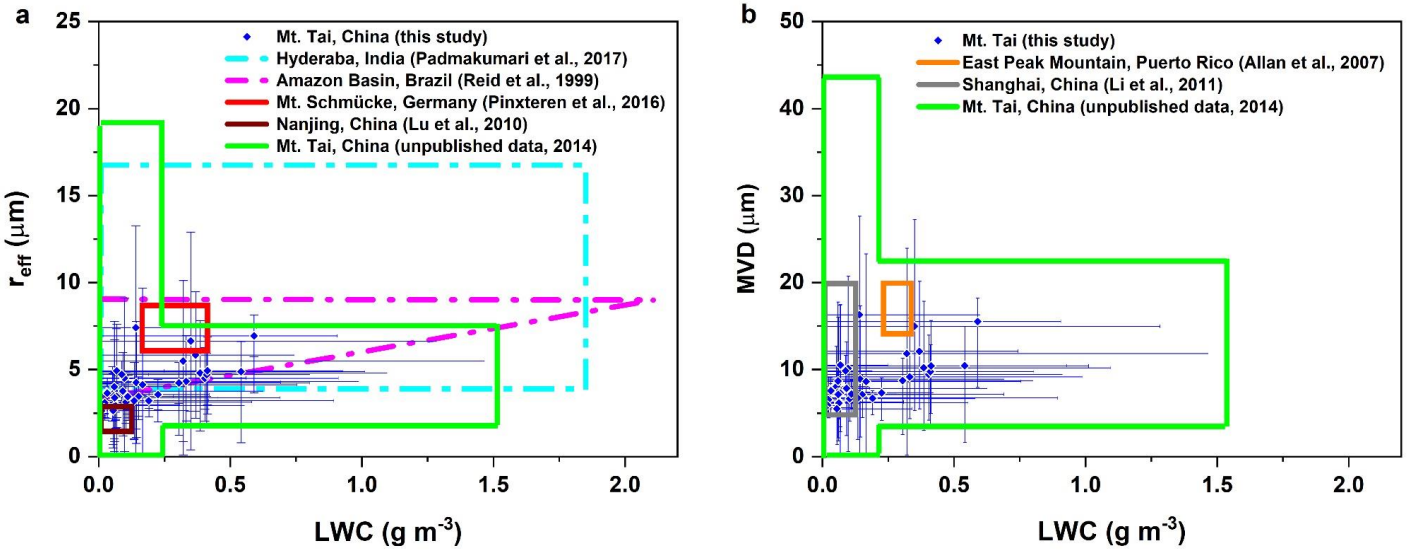

Figure 1: Plots of effective radius (r_{eff}, a) or medium volume diameter (MVD, b) against liquid water content (LWC) for clouds and fogs from the literatures. The dashed and solid shapes indicated the airborne and land observation, respectively. The blue diamonds with error bars represented the average LWC and r_{eff} (or MVD) of 40 cloud events observed at Mt. Tai in the present study with corresponding ranges

https://doi.org/10.5194/acp-2019-660
Preprint. Discussion started: 14 August 2019

Atmospheric Chemistry and Physics Discussions

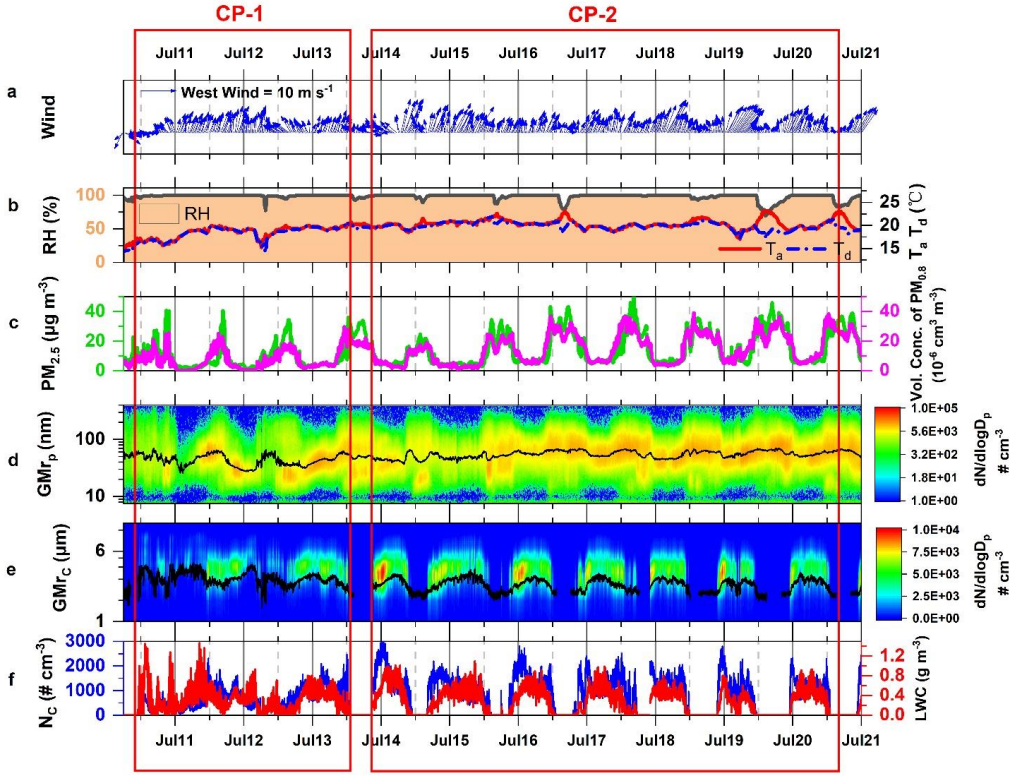

Figure 2: The monitoring information of CP-1 and CP-2. Including (a) Wind speed (WS, m s^{-1}) and wind direction (WD), (b) relative humidity (RH, %), ambient temperature (T_a, °C) and dew point temperature (T_d, °C) (c) $PM_{2.5}$ mass concentrations (μg m^{-3}) and volumn concentration of $PM_{0.8}$ (10^{-6} cm^3 cm^{-3}) (d) size distribution of particles (13.6-763.5 nm) and corresponding geometric mean radius (GMr_P) (e) size distribution of cloud droplets (2-50 μm) and corresponding geometric mean radius (GMr_C) (f) N_C and LWC of cloud droplets.

https://doi.org/10.5194/acp-2019-660
Preprint. Discussion started: 14 August 2019

Atmospheric Chemistry and Physics Discussions

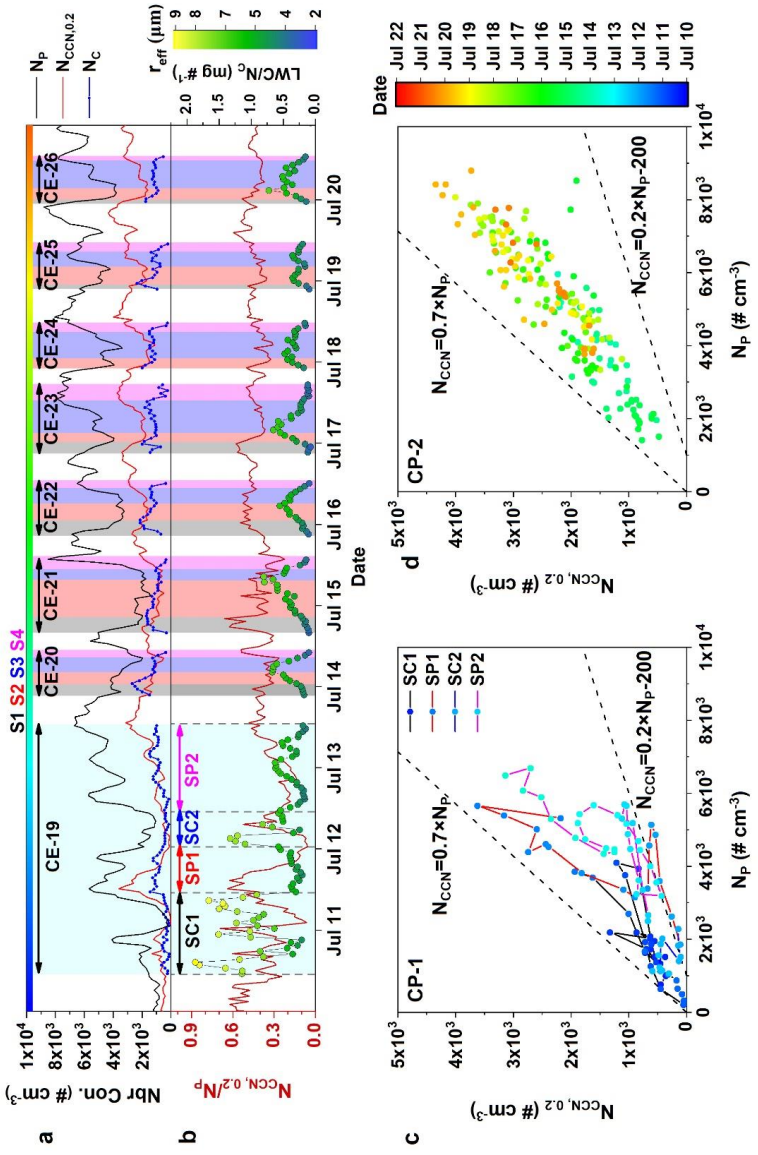

Figure 3: Variation of (a) N_C, N_P and $N_{CCN,0.2}$ (b) $N_{CCN,0.2}/N_P$ and LWC/N_C during CP-1 and CP-2. The plot of $N_{CCN,0.2}$ versus N_P (c) in CP-1 (d) in CP-2

https://doi.org/10.5194/acp-2019-660
Preprint. Discussion started: 14 August 2019

Atmospheric Chemistry and Physics Discussions

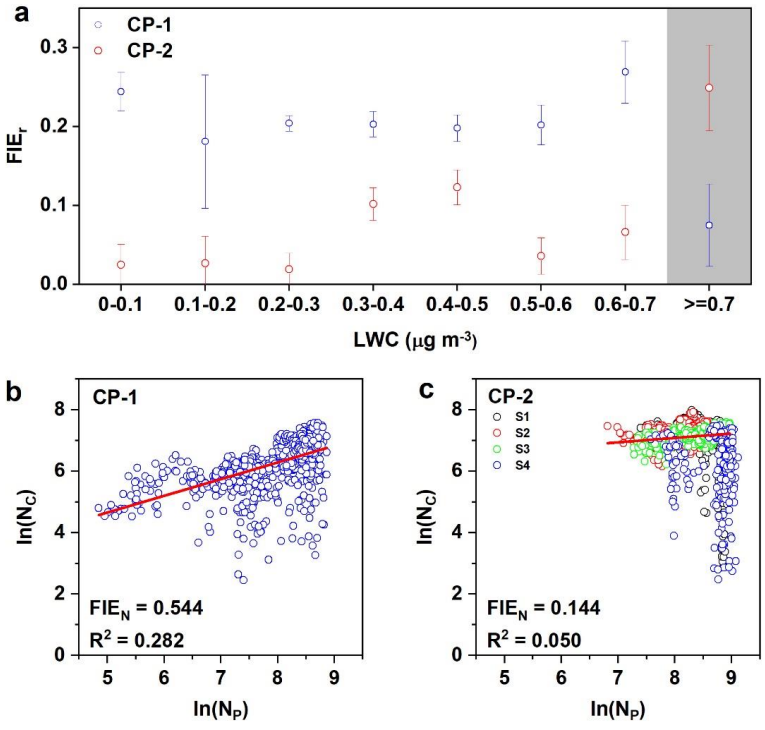

Figure 4: The determination of FIE (a) based on r_{eff} (b) and (c) based on N_C.

https://doi.org/10.5194/acp-2019-660
Preprint. Discussion started: 14 August 2019

Atmospheric Chemistry and Physics Discussions

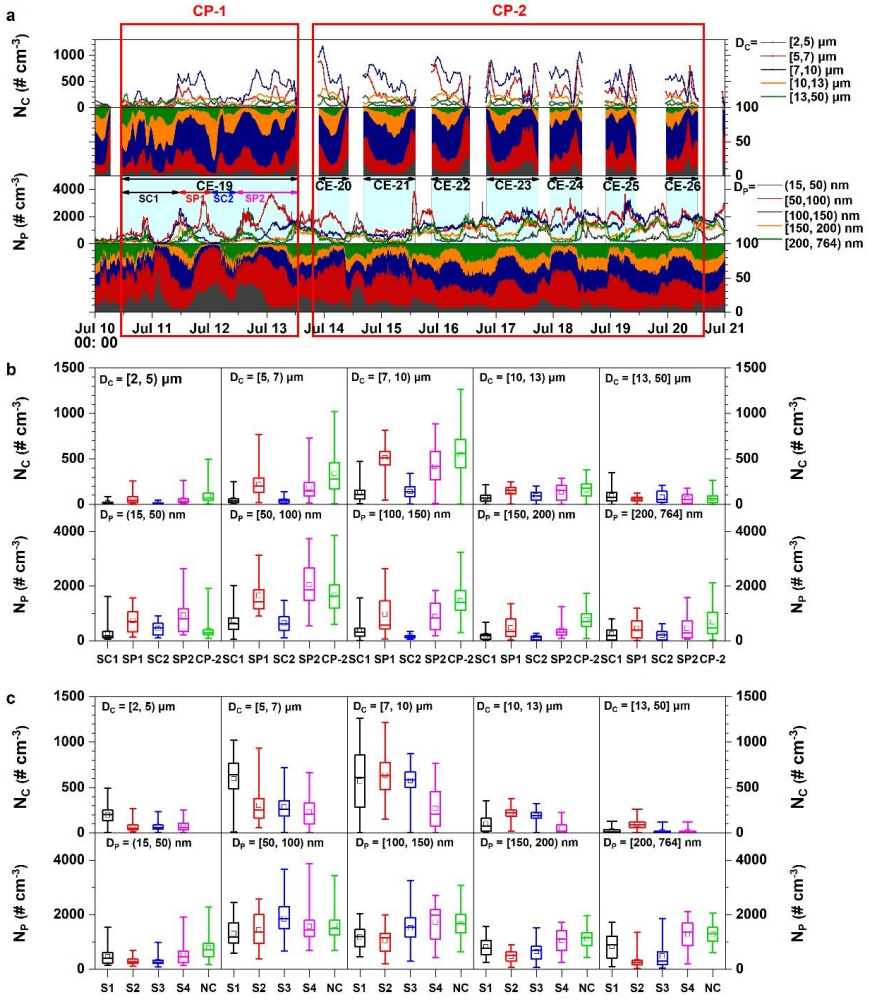

Figure 5: Size distribution of particles and cloud droplets during CP-1 and CP-2. "NC" in (c) represents particle size distributions during cloudless period

https://doi.org/10.5194/acp-2019-660
Preprint. Discussion started: 14 August 2019

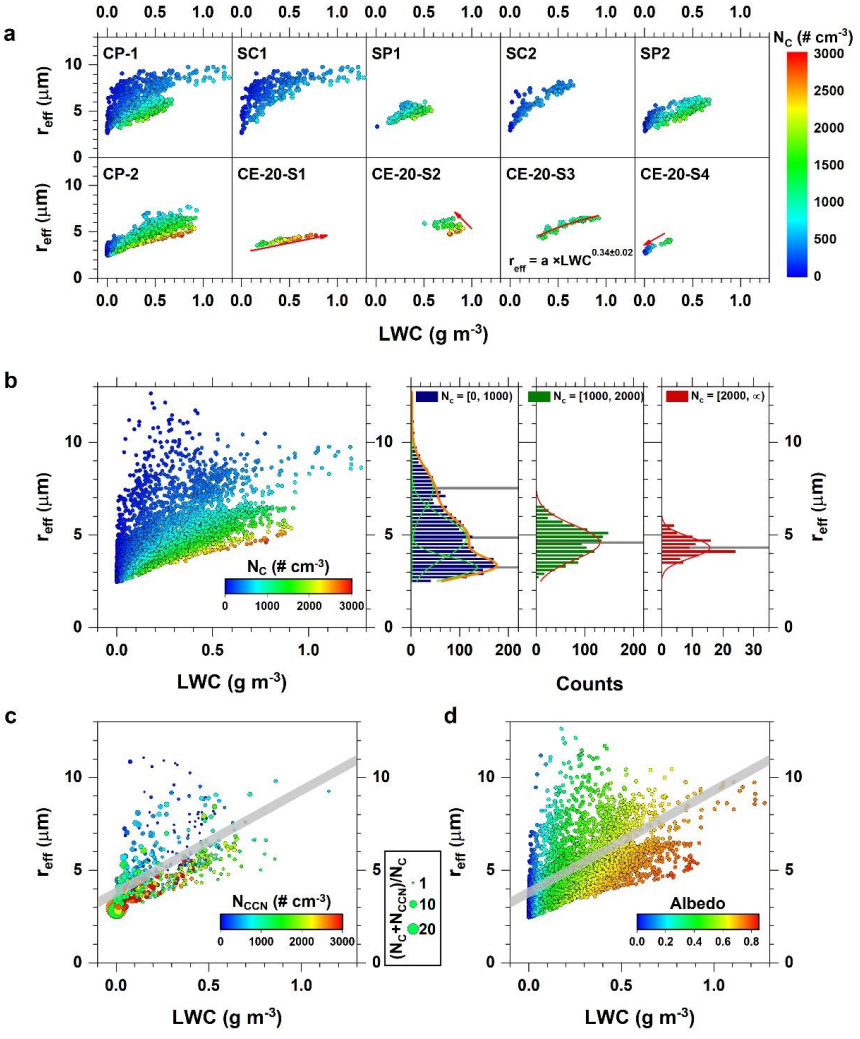

Figure 6: The plot of LWC versus r_{eff} (a) in CP-1 and in CP-2 (b) under different N_C ranges (c) under different N_{CCN} (d) with the variation of albedo.

https://doi.org/10.5194/acp-2019-660
Preprint. Discussion started: 14 August 2019

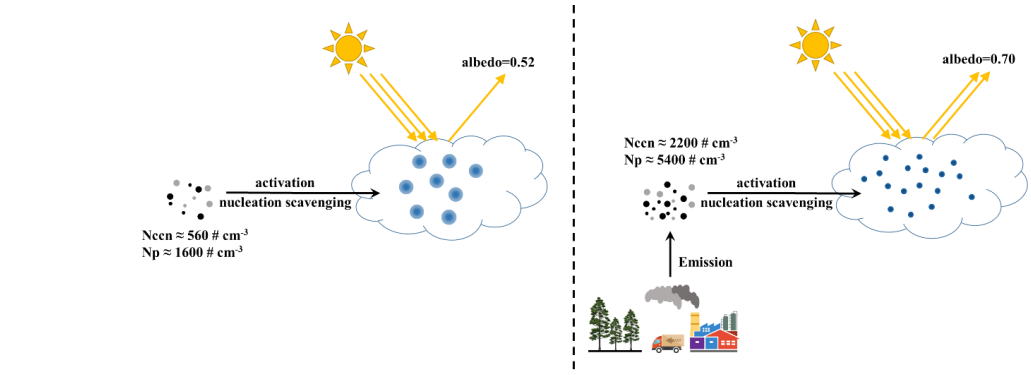

Figure 7: A schematic of cloud processes formed on different N_{CCN} and Np conditions.